Journal of Heat and Mass Transfer Research

Journal homepage: https://jhmtr.semnan.ac.ir

Semnan University

ISSN: 2383-3068

Research Article

Numerical Investigation of Thermohydraulic Performance in Laminar Flow through Microchannels Equipped with Longitudinal Vortex Generators

Zoubir Belkacemi [a *], Zakaria Boumahrat [b], Ahmed Dhiyaeddine Foul [b]

[a] *Departement of Physics, Faculty of Matter Sciences, Applied Energetic Physics Laboratory (LPEA), University of Batna 1, 05000 Batna, Algeria*

[b] *Department of Mechanical Engineering, Faculty of Technology Sciences, Constantine 1, Frères Mentouri University, Constantine 25000, Algeria*

ARTICLE INFO

Article history:

Received: 2024-12-10

Revised: 2025-05-26

Accepted: 2025-06-20

Keywords:

Fluid flow;

Heat transfer;

Laminar flow;

Microchannels;

Vortex generators.

ABSTRACT

Vortex generators (VGs) are widely employed to enhance heat transfer in channel flows by inducing vortices, with their performance strongly influenced by geometric parameters and flow conditions. This study numerically investigates the thermohydraulic performance of laminar flow (Re = 200–1200) in a rectangular microchannel (H = 0.26 mm) equipped with longitudinal vortex generators (LVGs) of reduced height (0.75H). The objective is to assess the impact of reduced LVG height on pressure loss and heat transfer enhancement, using water as the working fluid. Numerical simulations were validated against existing data, with deviations remaining below 10%, and were subsequently conducted for three LVG orientation angles (30°, 135°, and 150°). The results indicate that at Re = 1200, the LVGs increased the friction factor by up to 6% for 30° and 150° and 8% for 135°, while increasing the Nusselt number by up to 18% for 30° and 150° and 24% for 135°. The highest thermal performance factor of 1.21 was achieved at the 135° orientation for Re=1200, identifying it as the optimal configuration among those tested.

1. Introduction

In the last decade, the development of techniques to improve heat dissipation in mini/microdevices has gained increasing importance. This trend is driven by the critical need to maintain temperature balance for the long-term, efficient operation of modern technologies, especially in the cooling of electronic devices. Recognizing this significance, researchers have explored various approaches. These primarily involve first, designing novel configurations to optimize heat transfer, and second, using modified fluids with enhanced thermophysical properties, such as thermal conductivity and specific heat capacity. Numerous studies [1,2,3] have analyzed different heat sink shapes and channel geometries, consistently highlighting the significant influence of configuration on thermal enhancement across various flow regimes. Furthermore, these studies emphasize the concurrent effect of shape on

* **Corresponding author.**
E-mail address: zoubir.belkacemi@univ-batna.dz

Cite this article as:
Belkacemi, Z., Boumahrat, Z. and Foul, A. D., 2026. Numerical Investigation of Thermohydraulic Performance in Laminar Flow through Microchannels Equipped with Longitudinal Vortex Generators. *Journal of Heat and Mass Transfer Research*, 13(3), pp. 261-272.
https://doi.org/10.22075/JHMTR.2025.36208.1655

pressure loss, underscoring the opportunity for innovative configurations to achieve a better balance between heat transfer improvement and acceptable pressure drop. While the use of nanofluids with modified properties has also emerged as a prominent approach, their effectiveness often remains limited compared with configurational changes, particularly at lower volume fractions (1% to 5%) where improvements in the heat transfer coefficient closely align with increases in thermal conductivity relative to the base fluid [4].

Focusing on the configurational approach, the integration of vortex generators (VGs) into mini- and microchannels has become a key area in recent research due to their significant impact on thermohydraulic behavior. Numerous experimental studies have explored these effects. For instance, Chen et al. [5] examined microchannels (aspect ratios of 0.0667 and 0.25) equipped with longitudinal vortex generators (LVGs), finding heat transfer improvements of 12.3% to 73.8% and 3.4% to 45.5%, respectively, though accompanied by pressure loss increases of 158.6% and 47.7%. Similarly, Liu et al. [6] investigated the dynamic and thermal behavior in microchannels with varying numbers of LVG pairs and inclinations. Their work showed heat transfer enhancements of 9% to 21% for laminar flow and 39% to 90% for turbulent flow, again with significant pressure drops, and they notably observed an earlier transition to turbulence (Re = 600–730) due to the LVGs. In another study, Wang et al. [7] assessed LVG performance in rectangular channels for cooling nuclear fuel elements, reporting heat transfer improvements of 10%–45% and superior performance when LVGs were positioned on both sides of the channel compared with a single-sided configuration.

To further investigate fluid flow around vortex generators, combining numerical simulations with experimental studies has proven highly effective. Wang et al. [8], for example, conducted both experimental and numerical investigations on perforated curved-wing VGs mounted on opposing walls of a rectangular microchannel in turbulent flow (Re = 2500–3500). Using the SST k−ω turbulence model, they tested various opening angles and pitch ratios, concluding that these VGs enhanced heat transfer by inducing mixed vortices. In a subsequent study, Wang et al. [9] further explored the impact of VGs on thermal performance in turbulent channel flow, identifying hole shapes in punched VGs as key determinants of vortex configuration and strength. Their investigation of perforated curved rectangular winglet VGs in microchannels (Re = 2500–3500) also found that varying pitch and opening angle ratios significantly improved performance, yielding a thermal enhancement factor increase of up to 26%. Likewise, Srivastava et al. [10] utilized both numerical and experimental methods to analyze the effect of different VG shapes and geometric parameters. Their findings revealed that triangular VGs achieved the highest heat transfer coefficient for a selected orientation and pitch, while D-shaped VGs had their own optimal parameter set. Similarly, Sun et al. [11] numerically and experimentally investigated turbulent flow in circular tubes with multiple rectangular winglet VGs, examining parameters such as winglet number, height, and pitch, and reported Nusselt number enhancements of up to 2.32 times with a maximum thermal enhancement factor (TEF) of 1.27, also developing predictive correlations.

Given their efficiency, numerical simulations are now extensively used for designing configurations and assessing their effectiveness, further elucidating VG performance. Datta et al. [12] conducted a numerical study on MCHS equipped with LVGs (full height), demonstrating that optimal thermal performance occurred at a 30° LVG angle for Re > 600, while higher angles were better for Re < 600, also highlighting the influence of microchannel thickness. Fahad et al. [13] investigated novel VG shapes in turbulent rectangular channel flow (Re = 4000–11000), finding that a rectangular VG with three triangles on top yielded the highest Nusselt number increase (38.2%), though with an 80.38% friction factor increase; 30° for both vertical and horizontal inclinations proved optimal. Feng et al. [14] tested staggered triangular ribs in a laminar flow rectangular microchannel (H=W=0.2 mm), showing that rib geometric parameters significantly improved thermal performance, while their entropy generation analysis revealed configurations that reduced irreversibility. Building on such concepts, Sun et al. [15] studied microchannels with delta winglet VGs incorporating elliptical cylinders, numerically demonstrating Nusselt number enhancements from this combination ranging up to 14.9% over VGs alone, and a remarkable 63% increase compared to a smooth channel.

Further refining these numerical approaches, Zhang et al. [16] performed an optimization study using the Taguchi method for LVGs in a 3D microchannel, showing that longitudinal spacing and VG number strongly influenced the Nusselt number, achieving improvements of 23.6% in the Nu value and 7.2% in overall thermal efficiency. Ebrahimi et al. [17] assessed various LVG orientations and locations in laminar rectangular microchannel flow, finding Nusselt number improvements of 2% to 25% with a 4% to 30% increase in friction factor, attributing this to

enhanced fluid mixing. In a separate study on nanofluids, Ebrahimi et al. [18] showed that water-Al_2O_3 and water-CuO nanofluids (0.5%–3.0% volume fraction) enhanced heat transfer by 2.29%–30.63% and 9.44%–53.06%, respectively. Fu et al. [19] examined heat transfer in minichannels with delta winglet LVGs on opposite walls, finding that a "Mixed" configuration provided optimal heat transfer, improving Nusselt numbers by 28–35% compared with models without LVGs. Pérez et al. [20] numerically studied laminar flow in a rectangular duct with perforated VGs, finding that all tested configurations improved heat transfer by 12.8% but increased pressure loss by 17.5%, and notably observed a novel reverse vortex rotation. Reddy et al. [21] numerically examined baffle number and shape effects across a wide Reynolds number range (Re = 1800–22000), indicating that at lower Re, 30 V-shaped baffles achieved the highest Nusselt number due to intensified mixing, despite increased pressure loss. Demirag [22], in another numerical study, explored various VG geometric parameters in an asymmetrically heated duct (Re = 5000), achieving a maximum thermal enhancement factor (TEF) of 1.25.

Additionally, the combination of VGs with other complex geometries has gained significant interest. Zhang et al. [23] investigated integrating ribs with winglet and tetrahedral VGs in turbulent flow (Re = 20,000–100,000), demonstrating that winglet VGs with ribs outperformed other configurations, offering a 5.51% improvement in thermal performance over ribs alone. Salamatbakhsh et al. [24] analyzed laminar flow (Re = 500–1300) in a wavy minichannel with LVGs, finding that staggered LVGs yielded the best thermal performance factor (TPF) of 1.40–1.46, which was superior to the wavy channel without VGs.

Synthesizing these findings, including those from reviews like Bansode et al. [25], it is evident that both channel and VG configurations critically impact thermal performance. Geometric parameters such as pitch ratio and placement consistently play a crucial role, underscoring the importance of careful selection and overall design for optimizing thermohydraulic performance. Most research on enhancing heat transfer with LVGs emphasizes that key geometric parameters, including placement, height-to-width ratio, and orientation, are significant. Therefore, selecting appropriate geometric parameters for specific fluid conditions is crucial for achieving optimal configurations. The primary goal is often to reduce pressure loss while maintaining or improving heat transfer capacity. To this end, investigating the effect of reducing LVG height, making them smaller than the channel height, could offer valuable insights into their impact on both pressure loss and heat transfer, potentially mitigating the substantial pressure penalties associated with full-height VGs.

Building on previous work, particularly the findings of Liu et al. [6] on LVG inclinations and Ebrahimi et al. [17] on LVG orientations in microchannels, this study numerically investigates the effects of reduced-height LVGs on the thermohydraulic behavior of laminar fluid flow in a rectangular microchannel. Specifically, while Ebrahimi et al. [17] explored full-height LVGs, this study focuses on LVGs with a height equal to 75% of the microchannel height. Constant temperature boundary conditions are applied to both the upper and lower walls, and orientation angles similar to those in prior studies are explored, along with additional configurations, to broaden the analysis and identify optimal designs for this reduced-height parameter.

2. Physical Model and Numerical Method

Three-dimensional simulations were conducted on four configurations. The first configuration was a smooth microchannel, and for the three remaining models, longitudinal vortex generators were added to this base channel. In each of these LVG-equipped models, the height of the LVGs was maintained at three-quarters of H and oriented at three different angles (150°, 135°, and 30°), as illustrated in Figure 1. The LVGs were positioned within the entry length of the microchannel. The microchannel had a rectangular cross-section and the following dimensions: height (H) = 0.26 mm, length (L) = 39.37 mm, and width (W) = 5.25 mm.

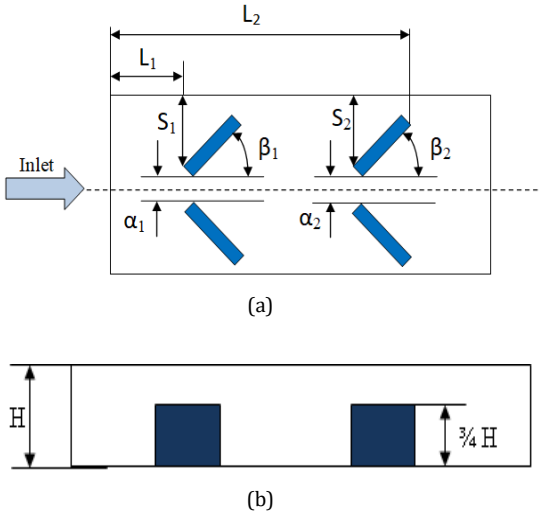

Fig. 1. Physical model: a) Top-view; b) Side-view.

Table 1 summarizes the geometric parameters defining the physical model. The layout configuration followed that of Ebrahimi et al. [17].

Table 1. Detailed geometric parameters

	L_1	L_2	α_1	α_2	s_1	s_2	β_1, β_2
Smooth Channel	-	-	-	-	-	-	-
LVG (150°)	50H	100H	4H	4H	8H	8H	150°, 150°
LVG (135°)	50H	100H	4H	4H	8H	8H	135°, 135°
LVG (30°)	50H	100H	4H	4H	8H	8H	30°, 30°

2.1. Governing Equations and Boundary Conditions

Throughout this study, water with constant thermophysical properties served as the coolant, and it was assumed to be a Newtonian, incompressible fluid. Several studies [26, 27] have reported conditions that support the persistence of laminar flow regimes around and over obstacles similar to those in the present model, which supports the current study's assumption of laminar, steady-state flow. Volume forces, viscous dissipation, and radiation effects were neglected.

Under these assumptions, the governing equations simplify as follows [28]:

$$\nabla.\vec{V} = 0 \tag{1}$$

$$\left(V.\nabla\vec{V}\right) = -\frac{1}{\rho}\nabla P + \mu\,\nabla^2\vec{V} \tag{2}$$

$$\rho C_p\left(\vec{V}\,.\nabla T\right) = \lambda\nabla^2 T \tag{3}$$

Numerous studies have identified water as an effective coolant due to its high thermal conductivity and specific heat capacity, and it has been consistently classified as a Newtonian fluid. Additionally, many studies [29, 30] have opted to assume constant fluid properties, often without addressing potential anomalies. Accordingly, all fluid properties are assumed to be constant in this study. The properties of water considered are summarized in Table 2.

Table 2. Fluid thermophysical properties [30]

Properties	**Water**
Density ρ	998.2 Kg/m^3
Heat capacity C_p	4182 $J/Kg\ K$
Thermal conductivity λ	0.6 $W/m\ K$
Dynamic Viscosity μ	1.003 x 10^{-3} $Kg/m\ s$
Temperature T	300 K

For the boundary conditions, a uniform velocity was applied at the channel inlet, with an imposed temperature of 300 K. A pressure was applied at the outlet, and a temperature of 350 K was imposed on the upper and lower walls. Adiabatic conditions were imposed on all remaining walls.

2.2. Numerical Approach and Characterized Parameters

Throughout the study, the commercial software ANSYS Fluent was used. A hybrid non-uniform grid was applied, with refined mesh sizes adjacent to all walls defining the model, including the longitudinal vortex generators, as shown in Figure 2. The convergence criterion was set to less than 10^{-6} for the momentum, continuity, and energy equations. For the velocity-pressure coupling, the SIMPLE algorithm was chosen. To interpret the numerical results, following physical parameters were defined.

The Reynolds number is defined as follows:

$$Re_{D_h} = \frac{\rho\ V\ D_h}{\mu} \tag{4}$$

where:

$$D_h = \frac{4\ H\ W}{2(H\ W)} \tag{5}$$

To quantify the ratio of convective and conductive heat transfer, the Nusselt number is calculated as follows:

$$Nu = \frac{h\ D_h}{k} \tag{6}$$

where:

$$h = \frac{Q}{(S\ \Delta T)} \tag{7}$$

$$Q = \dot{m}\ C_P\ (T_{out} - T_{in}) \tag{8}$$

The temperature difference was calculated using the logarithmic mean temperature difference (LMTD) equation:

$$\Delta T = \frac{(T_{wall}-T_{in})-(T_{wall}-T_{Out})}{\ln((T_{wall}-T_{in})-(T_{wall}-T_{Out}))} \quad (9)$$

The friction factor was calculated by the following relation:

$$f = \frac{2 \triangle P}{L} \frac{D_h}{\rho U^2} \quad (10)$$

The Poiseuille number quantifies the relationship between pressure drop and flow resistance and can be calculated using the following equation:

$$P_0 = Re\, f \quad (11)$$

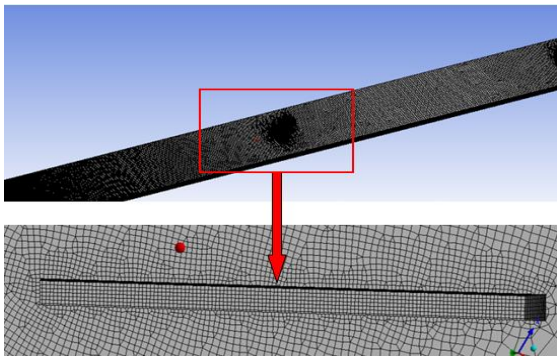

Fig. 2. Representative grid

2.3. Grid Independency and Validation

To achieve an optimal mesh, priority was given to element quality while minimizing the total number of elements to maintain a reasonable computation time. Three mesh tests were conducted, with the number of nodes incrementally increased in each test. Grid independence was evaluated by comparing the Nusselt number and friction factor values for each selected mesh size, as presented in Table 3.

Table 3. Grid independence test

Number of cells	***Nu***	***f***	***F* (Error %)**	***Nu* (Error %)**
319286	3.736261	0.05615922	------	------
612816	3.743363	0.05896718	0.05	0.19
879498	3.744112	0.05908512	0.002	0.02

To validate the current numerical model, its results were compared with the experimental data of Lui et al. [6] and the numerical results of Ebrahimi et al. [17].

The comparison focused on the friction factor and Nusselt number over a range of Reynolds numbers; this approach aligns with the current study's assumption of temperature-independent thermophysical properties and the applied thermal boundary conditions.

Figure 3 presents the comparative results. For the friction factor (Figure 3a), both qualitative and quantitative agreement were observed, with a maximum deviation of about 11% from the experimental data [6] and approximately 20% from the numerical results [17]. Notably, the experimental data [6] reported an uncertainty of 5.72%. The highest discrepancies occur at low Reynolds numbers (Re < 400), where conduction is dominant and viscosity variations due to temperature are more significant. These deviations decrease as Re increases, confirming the reduced influence of temperature-dependent properties at higher flow rates. Similar trends have been reported in previous studies [31], where adjusted formulations were proposed for low Reynolds number regimes.

For the Nusselt number (Figure 3b), the comparison showed good agreement, with deviations ranging from 6% to 15% relative to the experimental results [6], which are well within their reported uncertainty of 19.6%. A similar agreement was observed when comparing the present results with the numerical data from Ebrahimi et al. [17], with deviations between 6% and 12%. It is important to note that Nusselt number measurements typically involve higher uncertainties than those for the friction factor. Furthermore, differences in imposed boundary conditions across numerical studies can significantly influence heat transfer predictions, which partly explains these deviations. Overall, the discrepancies observed in the present results remain within acceptable margins, considering the reported experimental uncertainties, and do not compromise the predictive reliability of the numerical model.

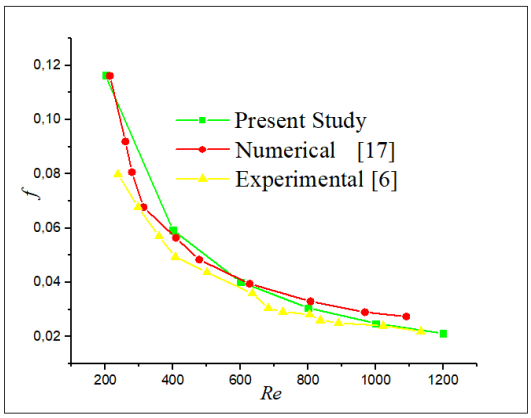

(a)

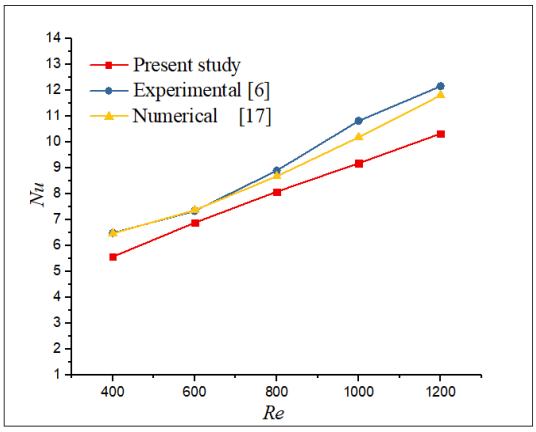

(b)

Fig. 3. Comparison of present results with experimental data and numerical results: (a) Friction factor; (b) Nusselt number

3. Results and Discussion

The temperature and velocity distributions, along with the calculated thermohydraulic parameters, allow for a deeper understanding of the effects of the LVGs on both the dynamic and thermal behavior of fluid flow. Therefore, the obtained results and their interpretations are divided into two sections. The first section addresses pressure loss, analyzed through the apparent friction factor, Poiseuille number, and velocity distribution along the microchannel. The second section focuses on the thermal behavior, examining the variation in the Nusselt number and the temperature distribution.

3.1. Dynamic Analysis of Flow Resistance

Figure 4 illustrates the variation of the friction factor with Reynolds number for the selected orientation angles. The friction factor for all microchannels equipped with LVGs is higher compared with that of the smooth microchannel, with this difference becoming more pronounced as the Reynolds number increases. The friction factors for the 150° and 30° orientations are nearly identical, while the friction factor for the 135° orientation is slightly higher. At low Reynolds numbers (Re = 200), the deviation relative to the smooth channel is around 1% and increases with the Reynolds number, reaching approximately 6% at Re = 1200 for the 30° and 150° orientations. In contrast, the 135° orientation shows a larger deviation, reaching approximately 8% at Re = 1200. Similar trends were reported by Lui et al. [6], who observed increasing deviations with Reynolds number, and by Ebrahimi et al. [17], who found even higher deviations, though still lower than those in [6].

These results confirm that microchannels with LVGs generate higher pressure losses due to flow–LVG interactions and increased flow resistance from the walls. LVGs disturb the flow by generating recirculation zones and vortices, which contribute to pressure loss. Additionally, the reduced distance between LVGs and the walls promotes flow detachment under adverse pressure gradients. The lower friction factor deviations observed in the present study, compared to those in the studies by Liu et al. [6] and Ebrahimi et al. [17], are likely due to the selected LVG height of 0.75H. This reduced height decreases the constriction effect and allows smoother flow above the LVGs.

The analysis also highlights the influence of orientation angles on friction factor behavior. The 30° and 150° angles, being mirrored orientations, induce similar flow structures and thus produce comparable pressure losses. In contrast, the 135° orientation generates larger vortices and a more reduced constricted distance to the walls, resulting in greater pressure loss; this is consistent with observations by Liu et al. [6]. To further explore the effects of LVGs and their orientations on fluid dynamics, the next section examines variations in the Poiseuille number and the velocity distributions.

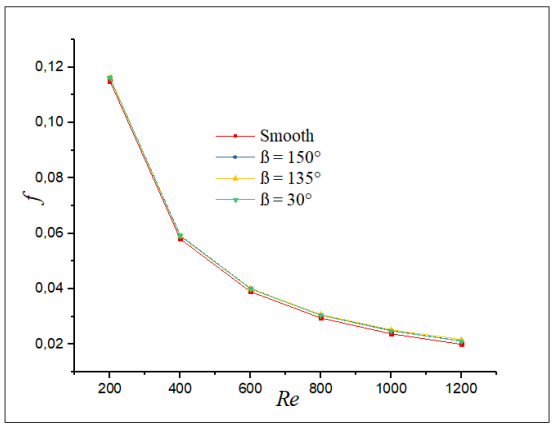

Fig. 4. Variation of the friction factor as a function of Reynolds number

The Poiseuille number quantifies dimensionless pressure loss and reflects boundary layer stability in laminar flow. While it remains relatively constant for smooth microchannels, the Poiseuille number typically varies in channels with disturbances, such as roughness or obstacles, due to induced vortex formation and flow detachment [32, 33].

Figure 5 presents the Poiseuille number as a function of the Reynolds number, showing an increase in this number with the Reynolds number for channels equipped with LVGs. This variation is influenced by LVG orientation angles, making the Poiseuille number a clear indicator of flow disturbances.

Similar to the friction factor behavior, the 30° and 150° orientations produce nearly identical

effects on pressure loss, indicating comparable flow behavior. In contrast, the 135° orientation induces significantly greater pressure loss, particularly beyond Re = 800. This effect is due to the reduced constricted distance between the channel walls and LVGs at the 135° orientation, causing stronger adverse pressure gradients, flow detachment, and the formation of larger local vortices. These detachments interrupt the boundary layer development along the flow direction. The constriction also forces local flow acceleration, followed by more rapid deceleration and expansion downstream, thereby intensifying the adverse pressure gradients.

To further understand the impact of LVGs on flow dynamics, the velocity distribution along the microchannel is subsequently examined. Building upon the friction factor and Poiseuille number analyses, this examination provides a more comprehensive view of the fluid behavior.

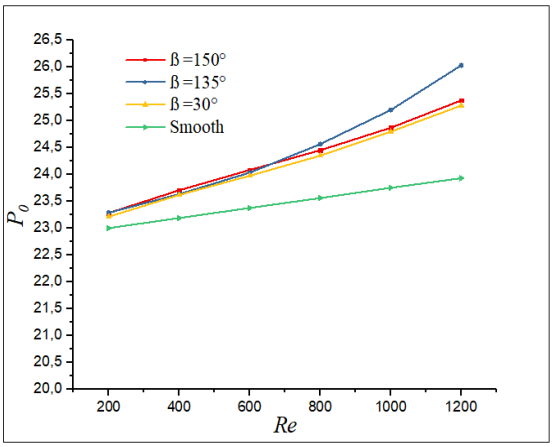

Fig. 5. Variation of the Poiseuille number as a function of Reynolds number

Figure 6 illustrates the velocity contours for the different LVG orientation angles at Reynolds numbers Re = 600 and Re = 1200. These contours clearly show the velocity distribution around the LVGs, showing the generation of both local and downstream longitudinal vortices. An increase in the Reynolds number produces larger local vortices in the immediate wake region of the LVGs and more pronounced downstream vortices, especially for the 135° orientation.

Additionally, the velocity contours confirm that the 30° and 150° orientations have a similar impact on fluid flow, as both induce comparable vortex structures.

Overall, these results emphasize the dominant role of both local and longitudinal vortices in enhancing heat transfer by enlarging the vortex area and intensifying fluid mixing with increasing Reynolds number.

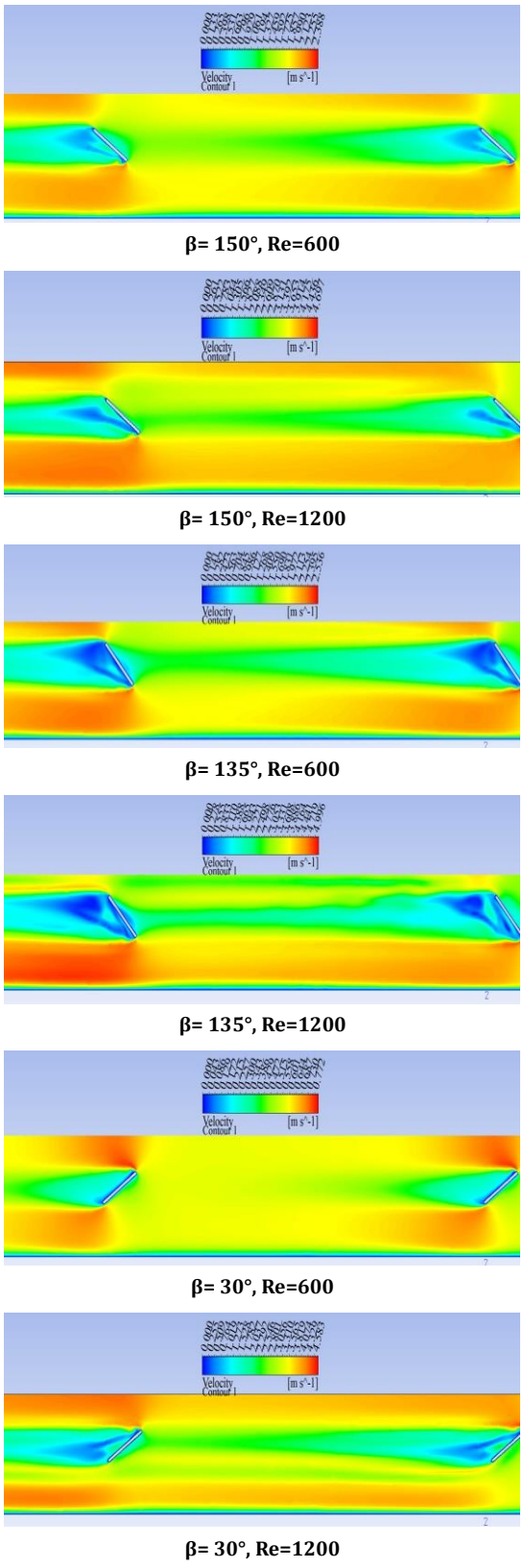

β= 150°, Re=600

β= 150°, Re=1200

β= 135°, Re=600

β= 135°, Re=1200

β= 30°, Re=600

β= 30°, Re=1200

Fig. 6. Contour of velocity distribution (Z=3/8H)

3.2. Thermal Analysis of Heat Transfer Enhancement

Figure 7 illustrates the variation of the Nusselt number with the Reynolds number for microchannels equipped with differently

oriented LVGs. The results confirm that LVGs significantly enhance heat transfer, primarily through enhanced convective mechanisms (advection), with the orientation angle playing a critical role. Notably, the Nusselt number in LVG-equipped microchannels exceeds that of a smooth channel for Reynolds numbers above approximately 400, and this advantage becomes more pronounced as the Reynolds number increases. Quantitatively, the 150° and 30° orientations exhibit a Nusselt number enhancement (relative to the smooth channel) that increase from approximately 6% at Re = 600 to approximately 18% at Re = 1200. In comparison, the 135° orientation shows an even greater improvement, with enhancement ranging from approximately 7% to approximately 24% over the same Reynolds number range, highlighting the strong influence of the Reynolds number on thermal performance.

This improvement is primarily attributed to vortex dynamics: higher Reynolds numbers induce greater disturbance of the thermal boundary layers, leading to the formation of local (wake) and longitudinal vortices downstream of the LVGs. The disruption of these boundary layers promotes the development of secondary flows (longitudinal vortices), which improve fluid mixing and, consequently, heat transfer between the fluid and the channel walls. Furthermore, the degree of flow constriction caused by the LVG orientation significantly affects both the fluid dynamics and the thermal behavior by promoting flow separation and increasing vorticity generation. This suggests that configurations producing greater constriction may be more effective for heat transfer enhancement. Nevertheless, further investigation into the combined effects of constriction and inclination is recommended.

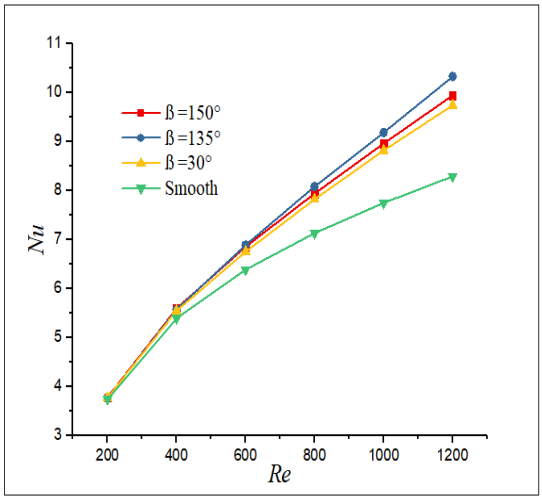

Fig. 7. Variation of the Nusselt number as a function of Reynolds number

Figure 8 displays the temperature distribution contours on the (x, y) plane at Z = 3/8H, highlighting the influence of both local and longitudinal vortices on heat transfer enhancement. Local vortices are especially prominent for the 135° LVG orientation and become more pronounced with increasing Reynolds number. Longitudinal vortices appear across all configurations and intensify as the Reynolds number rises, due to stronger boundary layer disturbances that generate larger and more energetic secondary flows. With the LVGs maintained at a constant temperature, their interaction with the flow disturbs the thermal boundary layers, initiating vortex formation and enhancing heat transport via advection. Importantly, the specific LVG configuration (e.g., angle, shape) dictates the nature of this fluid-surface interaction and the resulting vortex structures, thereby strongly influencing the effectiveness of local heat transfer enhancement near the LVGs. Furthermore, the LVG surfaces themselves contribute directly to heat transfer, acting as additional heat sources alongside the channel walls.

The temperature field reveals that near the first pair of LVGs, heat transfer is concentrated around the LVG surfaces due to local vortices, while longitudinal vortices gradually transport heat downstream. By the time the flow reaches the second LVG pair, longitudinal vortices dominate, enhancing mixing and heat transfer further. Therefore, while longitudinal vortices play a significant role, the contribution of local vortices near the LVG surfaces—strongly dependent on the LVG configuration—is also substantial. Attributing the enhancement solely to longitudinal vortices oversimplifies the underlying heat transfer mechanism. Further analysis is needed to quantify the distinct roles of both vortex types in the overall thermal performance.

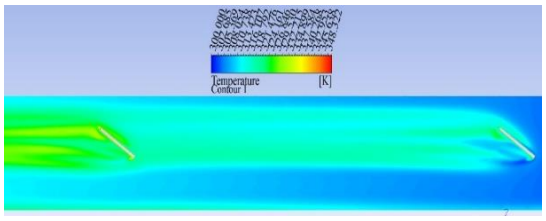

β= 150°, Re=600

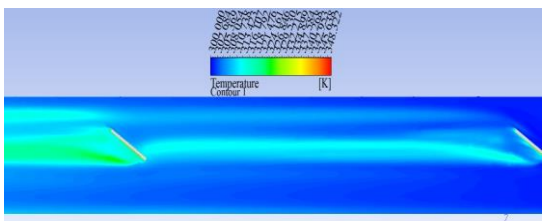

β= 150°, Re=1200

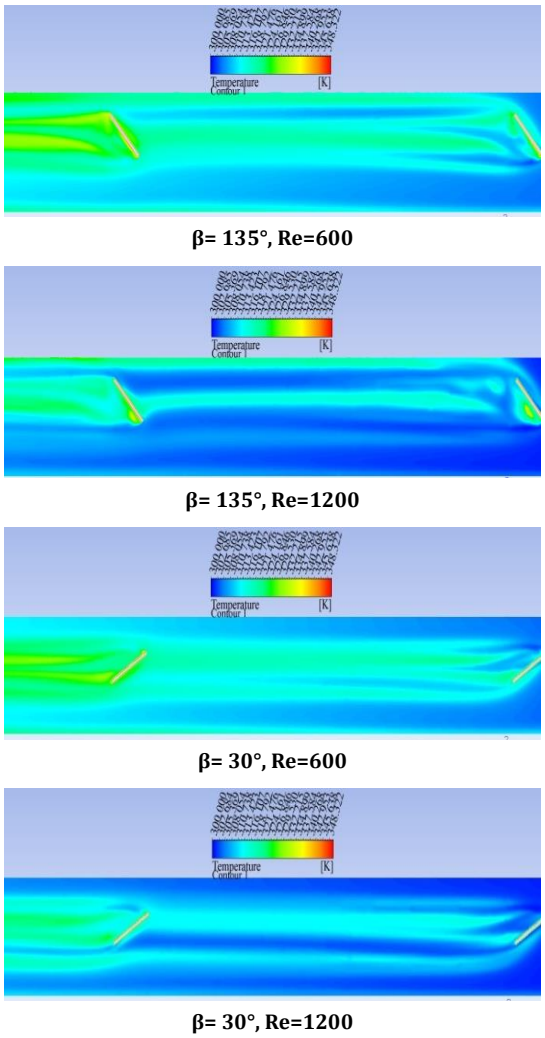

Fig. 8. Contour of temperature distribution (Z=3/8H)

3.3. The Overall Heat Transfer Enhancement

Heat transfer enhancement is strongly correlated with pressure loss, as indicated by the augmentation of the friction factor. Therefore, incorporating additional parameters to further quantify the relationship between heat transfer enhancement and pressure loss, or to highlight optimal configurations, is highly recommended. To assess overall thermal efficiency, the following parameters are defined [34]:

$$\eta_{Nu} = \frac{Nu}{Nu_s} \quad (12)$$

$$\eta_f = \frac{f}{f_s} \quad (13)$$

$$\eta_{th} = \frac{\eta_{Nu}}{\eta_f{}^{1/3}} \quad (14)$$

Here, η_{Nu} and η_f represent the ratios of the Nusselt number and friction factor for microchannels equipped with LVGs to those for a smooth channel, respectively. η_{th} represents the thermal performance factor or thermal efficiency. Figure 9 shows the variation of parameters characterizing the thermal and hydrodynamic efficiency for the studied configurations across different Reynolds numbers. From figure 9, it is evident that the optimal thermal performance factor reaches 1.21 for the 135° orientation angle at a Reynolds number of 1200. Notably, the thermal performance factor achieved in this study exceeds that reported by [17], reflecting a greater enhancement in heat transfer relative to pressure loss. The chosen configuration, with a 135° orientation angle and reduced height, optimizes heat transfer more effectively than LVGs with full channel height. For other configurations, heat transfer improvement remains consistently higher than that reported by [17], highlighting the role of the reduced height in minimizing pressure loss.

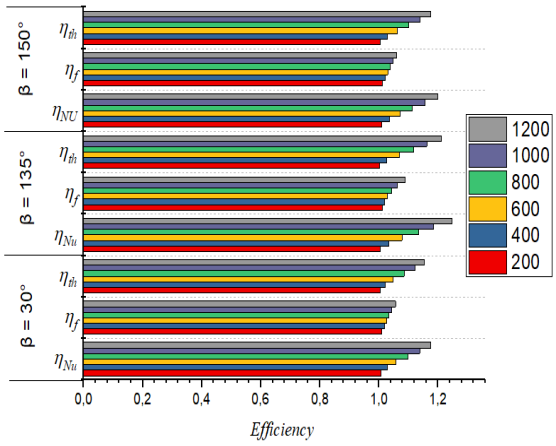

Fig. 9. Effect of orientation angles on thermal and dynamic efficiency

Table 4 compares the overall thermal performance from the present laminar flow study against three previous investigations. Within the laminar regime for microchannels equipped with LVGs, the results confirm that reduced-height configurations achieve superior overall thermal performance compared to their full-height counterparts reported in the literature. For context, the performance achieved in this laminar study is also compared with results from one turbulent flow investigation, illustrating that turbulent regimes, as expected, provide significantly higher overall thermal performance.

Table 4. Comparison of overall thermal performance between present study and literature

	Present Study	Ebrahimi et al. [17]	Datta et al. [12]	Liu et al. [6]	
Overall thermal performance (η_{th})	1.21	1.14	1.18	Laminar flow	Turbulentflow
				1	1.37

4. Conclusions

This study numerically investigates the influence of longitudinal vortex generators (LVGs) on the thermal and hydrodynamic characteristics of laminar flow in rectangular microchannels. The configurations analyzed consist of two pairs of LVGs symmetrically mounted on the lower walls of the channels, oriented at three distinct angles (30°, 135°, and 150°) and with a reduced height (3/4H) relative to the channel height. Three-dimensional simulations were performed using Fluent software, to capture detailed insights into the flow and heat transfer behavior. The results obtained were validated against available data in the literature, demonstrating good agreement with both experimental and numerical findings. The conclusions drawn from this study are as follows:

- For microchannels equipped with LVGs, within the Reynolds number range of 200 to 1200, the friction factor increases by 1-8% compared to smooth channels, with this increase remaining lower than that reported in the literature for full-height LVGs.
- The increase in friction factor was attributed to local and longitudinal vortices generated by the LVGs, as well as flow detachment around the LVG structures.
- Friction factor deviations increase with Reynolds number, reaching a maximum at the highest values of Reynolds.
- Fluid disturbances were influenced by orientation angles, with the largest friction factor deviation observed at a 135° orientation.
- Across all Reynolds numbers from 200 to 1200, the Nusselt number for LVG-equipped microchannels increases by 7% to 24%, with the highest enhancement (24%) occurring at a 135° orientation and Reynolds number of 1200. For the other angles, heat transfer enhancement was approximately 18% at the same Reynolds number.
- This heat transfer improvement was attributed to the generation of local and longitudinal vortices by the LVG configurations.
- The constricted distance between LVGs, and between LVGs and walls, affected local vortex generation, leading to further enhancement in combination with LVG height and orientation.
- LVG height influenced friction loss, with reduced LVG heights demonstrating lower pressure loss and comparable heat transfer enhancement to that of full-height LVGs.
- The overall thermal performance was highest for the 135° orientation, with a thermal performance factor of 1.21. For the other two angles, this factor reached approximately 1.16.

This study elucidates the mechanisms by which longitudinal vortex generators (LVGs) enhance heat transfer within microchannels. The results demonstrate that LVG configuration, particularly shape, orientation, and placement, has a significant influence on vortex generation and, consequently, on thermal performance. Further research should focus on exploring innovative configurations, such as sinusoidal shapes and asymmetric orientations, as well as on quantifying the individual contributions of local and longitudinal vortices. Such efforts would address key knowledge gaps and facilitate the design of optimized LVG configurations for enhanced heat transfer.

Nomenclature

S	Contact surface, m^2
Cp	Specific heat, J kg^{-1} K^{-1}
D_h	Hydraulic diameter, m
f	Friction factor
h	Heat transfer coefficient, Wm^{-2} K^{-1}
H	Depth of the microchannel, m
λ	Thermal conductivity, Wm^{-1} K^{-1}
L	Length of the microchannel, m
$\dot{m}$	Mass flow rate, $kg\ s^{-1}$
MCHS	Microchannel heat sinks
Nu	Nusselt number
P	Static pressure, Pa
Po	Poiseuille number
Q	Heat flux, Wm^{-2}
Re	Reynolds number
T	Temperature, K
V	Velocity, m s^{-1}
W	Width of microchannel, m
Δp	Pressure drop, Pa
LVG	Longitudinal vortex generator
VG	Vortex generator

Greek and Latin letter

η	Efficiency
ρ	Density, kg m^{-3}
μ	Dynamic viscosity, Pa s

Subscripts

in	Inlet
out	Outlet
Wall	Surface wall

Funding Statement

This research did not receive any specific grant from funding agencies in the public, commercial, or not-for-profit sectors.

Conflicts of Interest

The author declares that there is no conflict of interest regarding the publication of this article.

Authors Contribution Statement

Zoubir Belkacemi: Conceptualization; Data Curation; Formal Analysis; Methodology; Project Administration; Validation; Writing – original draft; Writing – review & editing.

Zakaria Boumahrat: Data Curation; Formal Analysis; Software; Validation; Writing – review & editing.

Ahmed Dhiyaeddine Foul: Data Curation; Formal Analysis; Software; Validation; Writing – review & editing.

References

[1] Dharaiya, V. V. and Kandlikar, S. G., 2012. Numerical investigation of heat transfer in rectangular microchannels under H2 boundary condition during developing and fully developed laminar flow. *Journal of Heat Transfer*, 134, 020911.

[2] Khoshvaght-Aliabadi, M., Hosseinirad, E., Farsi, M. and Hormozi, F., 2021. Heat transfer and flow characteristics of novel patterns of chevron minichannel heat sink: An insight into thermal management of microelectronic devices. *International Communications in Heat and Mass Transfer*, 122, 105044.

[3] Ajeel, R. K., Salim, W. S. I. W. and Hasnan, K., 2020. Numerical investigations of heat transfer enhancement in a house-shaped corrugated channel: Combination of nanofluid and geometrical parameters. *Thermal Science and Engineering Progress*, 17, 100376.

[4] Buschmann, M. H., Azizian, R., Kempe, T., Juliá, J. E., Martínez-Cuenca, R., Sundén, B., Wu, Z., Seppälä, A. and Ala-Nissila, T., 2018. Correct interpretation of nanofluid convective heat transfer. *International Journal of Thermal Sciences*, 129, pp. 504-531.

[5] Chen, C., Teng, J.-T., Cheng, C.-H., Jin, S., Huang, S., Liu, C., Lee, M.-T., Pan, H.-H. and Greif, R., 2014. A study on fluid flow and heat transfer in rectangular microchannels with various longitudinal vortex generators. *International Journal of Heat and Mass Transfer*, 69, pp. 203–214.

[6] Liu, C., Teng, J., Chu, J.-C., Chiu, Y.-L., Huang, S., Jin, S., Dang, T., Greif, R. and Pan, H.-H., 2011. Experimental investigations on liquid flow and heat transfer in rectangular microchannel with longitudinal vortex generators. *International Journal of Heat and Mass Transfer*, 54(13), pp. 3069-3080.

[7] Wang, Q., Chen, Q., Wang, L., Zeng, M., Huang, Y. and Xiao, Z., 2007. Experimental study of heat transfer enhancement in narrow rectangular channel with longitudinal vortex generators. *Nuclear Engineering and Design*, 237(7), pp. 686–693.

[8] Wang, J., He, Y., Zeng, L., Liu, Z., Li, C. and Dou, J., 2024. Thermohydraulic performance intensification in a rectangular channel using punched vortex generators. *International Communications in Heat and Mass Transfer*, 157, 107799.

[9] Wang, J., Zeng, L. and He, Y., 2024. Thermal performance augmentation of microchannel using curved rectangular winglet vortex generators having rectangular perforation. *Chemical Engineering Science*, 24, pp. 01160-6.

[10] Srivastava, K. and Sahoo, R. R., 2024. Experimental and numerical study on thermal performance of new envelope and triangular vortex generators with different pitch and angle of attack. *Thermal Science and Engineering Progress*, 49, 102459.

[11] Sun, Z., Zhang K., Li, W., Chen, Q. and Zheng, N., 2020. Investigations of the turbulent thermal-hydraulic performance in circular heat exchanger tubes with multiple rectangular winglet vortex generators. Applied Thermal Engineering, 168, 114838.

[12] Datta, A., Sanyal, D. and Das, A. K., 2016. Numerical investigation of heat transfer in microchannel using inclined longitudinal vortex generator. *Applied Thermal Engineering*, 108, pp. 1008–1019.

[13] Fahad, M. K., Ifraj, N. F., Tahsin, S. H. and Hasan, M. J., 2023. Numerical investigation of the hydrothermal performance of novel vortex generators in a rectangular channel by employing inclination and rotational angles. *International Journal of Thermofluids*, 20, 100500.

[14] Feng, Z., Zhou, C., Guo, F., Zhang, J., Zhang, Q. and Li, Z., 2023. The effects of staggered triangular ribs induced vortex flow on hydrothermal behavior and entropy generation in microchannel heat sink.

International Journal of Thermal Sciences, 191, 108331.

[15] Sun, H., Fu, H., Ma, H., Sun, T., Luan, Y. and Zunino, P., 2024. Heat transfer enhancement mechanism of elliptical cylinder for minichannels with delta winglet longitudinal vortex generators. *International Journal of Thermal Sciences*, 198, 108839.

[16] Zhang, J.-F., Jia, L., Yang, W.-W., Taler, J. and Oclon, P., 2019. Numerical analysis and parametric optimization on flow and heat transfer of a microchannel with longitudinal vortex generators. *International Journal of Thermal Sciences*, 141, pp. 211-221.

[17] Ebrahimi, A., Roohi, E. and Kheradmand, S., 2015. Numerical study of liquid flow and heat transfer in rectangular microchannel with longitudinal vortex generators. *Applied Thermal Engineering*, 75, pp. 576-583.

[18] Ebrahimi, A., Rikhtegar, F., Sabaghan, A. and Roohi, E., 2016. Heat transfer and entropy generation in a microchannel with longitudinal vortex generators using nanofluids. *Energy*, 101, pp. 190-201.

[19] Fu, H., Sun, H., Yang, L., Yan, L., Luan, Y. and Magagnato, F., 2023. Effects of the configuration of the delta winglet longitudinal vortex generators and channel height on flow and heat transfer in minichannels. *Applied Thermal Engineering*, 227, 120401.

[20] Pérez, B, R., Menéndez Pérez, A. and Sacasas Suárez, D., 2022. Influence of the punched holes on thermohydraulic performance and flow pattern of rectangular channels with a pair of perforated vortex generators. *International Journal of Heat and Mass Transfer*, 184, 122191.

[21] Reddy, P. N., Verma V., Kumar A. and Awasthi M. K., 2023. CFD Simulation and Thermal Performance Optimization of Channel Flow with Multiple Baffles. *Journal of Heat and Mass Transfer Research*, 20, pp. 257- 268.

[22] Demirağ H. Z., 2025. The impact of vortex generator positioning and heated surface orientation on thermal performance and flow dynamics in asymmetrically heated duct. *Case Studies in Thermal Engineering,* 70, 106075.

[23] Zhang, G., Liu, J. and Sundén, B., 2021. Combined experimental and numerical studies on flow characteristic and heat transfer in ribbed channels with vortex generators of various types and arrangements. *International Journal of Thermal Sciences*, 167, 107036.

[24] Salamatbakhsh, E. and Bayer, Ö., 2024. Hydrothermal performance of a wavy minichannel heat sink with longitudinal vortex generators. *Thermal Science and Engineering Progress*, 50, 102506.

[25] Bansode, V. H., Verma, M., Naik, C. K., Pandhare, A., Anjinappa, C. , Prakash, C., Mohammed, S. J., Majdi, H. S. and Majdi, A., 2024. Air-side heat transfer enhancement using vortex generators on heat transfer surfaces- A comprehensive review, Journal of Heat and Mass Transfer Research, 22, pp. 255-272.

[26] Brackbill, T. P. and Kandlikar, S. G., 2007. Effect of sawtooth roughness on pressure drop and turbulent transition in micro-channels. *Heat Transfer Engineering*, 28(9), pp. 662-669.

[27] Ferrouillat, S., Tochon, P., Peerhossaini, H. and Garnier, J., 2006. Intensification of heat-transfer and mixing in multifunctional heat exchangers by artificially generated streamwise vorticity. *Applied Thermal Engineering*, 26(16), pp. 1820-1829.

[28] White, F. M. 2016. *Fluid Mechanics* (8th ed.). New York: McGraw-Hill.

[29] Fu, H., Sun, H., Yang, L., Yan, L., Luan, Y. and Magagnato, F., 2023. Effects of the configuration of the delta winglet longitudinal vortex generators and channel height on flow and heat transfer in minichannels. *Applied Thermal Engineering*, 227, 120401.

[30] Wu, X., Fu, T., Wang, J., Zeng, L. and Zhang, F., 2024. A comparative study of fluid flow and heat transfer in the tube with multi-V-winglets vortex generators. *Applied Thermal Engineering*, 236, 121448.

[31] Kays, W. M. and London, A. L., 1984. *Compact Heat Exchangers*. McGraw-Hill, New York, NY, pp. 105, 112.

[32] Webb, R. L., Eckert, E. R. G. and Goldstein, R. J., 1971. Heat transfer and friction in tubes with repeated-rib roughness. *International Journal of Heat and Mass Transfer*, 14(4), pp. 601-614.

[33] Croce, G. and D'Agaro, P., 2004. Numerical analysis of roughness effect on micro-tube heat transfer. *Superlattices and Microstructures*, 35, pp. 601–616.

[34] Bi, C., Tang, G. H. and Tao, W. Q., 2013. Heat transfer enhancement in mini-channel heat sinks with dimples and cylindrical grooves. *Applied Thermal Engineering*, 55(1–2), pp. 121–132.